# High power diode-side-pumped 1 112-nm Nd:YAG laser based on master-oscillator power-amplifier system

**Biaolong Liu (刘飙龙)[1,3], Zhichao Wang (王志超)[1*], Feng Yang (杨 峰)[1], Zhimin Wang (王志敏)[1], Yong Bo (薄 勇)[1], Hongtao Yuan (袁宏韬)[1], Lei Yuan (袁 磊)[1], Baoshan Wang (王保山)[1], Jialin Xu (许家林)[1], Yading Guo (郭亚丁)[1], Qinjun Peng (彭钦军)[1], Jingyuan Zhang (张景园)[2], Dafu Cui (崔大复)[1], and Zuyan Xu (许祖彦)[1**]**

[1] *Research Centre for Laser Physics and Technology, Key lab of Functional Crystal and Laser Technology, Technical Institute of Physics and Chemistry, Chinese Academy of Sciences, Beijing 100190, China*

[2] *Department of Physics, Georgia Southern University, Statesboro, Georgia 30460, USA*

[3] *University of Chinese Academy of Sciences, Beijing 100190, China*

[*] *Corresponding author: cationhaigou@163.com;* [**] *corresponding author: zyxu@mail.ipc.ac.cn*

Received November 11, 2013; accepted January 22, 2014; posted online February 28, 2014

We demonstrate a high power high beam quality diode-pumped 1 112-nm Nd:YAG master-oscillator power-amplifier (MOPA) laser system. To increase the extraction efficiency and output power, a four-pass amplifier scheme is employed. Finally, the injected laser output power is amplified from 26 to 64 W with beam quality factor $M^2$=2.85. Furthermore, a theoretical model that takes the temporal overlap inversion number dynamics into account is employed to analyze the performance of the MOPA laser system, and a good agreement with the experimental data is obtained.

*OCIS codes:* 140.3280, 140.3538, 140.3480.

*doi: 10.3788/COL201412.031404.*

Diode-pumped high power Nd:YAG lasers operating around 1.1 $\mu$m are always the most attractive laser system desired in remote monitoring, chemical testing, and nonlinear optical harmonic generation and etc.[1−12]. Especially, the 1112-nm lasers can be applied in selecting photo-ionization in laser chemistry[13] and used as a pump source for thulium up-conversion fiber lasers to produce blue laser emission[14]. Moreover, the yellow-green and ultraviolet (UV) lasers can be generated through second harmonic generation (SHG) and fourth harmonic generation (FHG) of 1112-nm lasers, which have many attractive applications in laser display, atmospheric remote sensing, medical treatment, laser precision manufacture, and bio-analysis fields[15−20].

In the earlier reports, the investigations of 1.1-$\mu$m lasers were mainly focused on diode-end-pumped structure[1−8,13−16]. For example, using a standing-wave laser configuration and diode-end-pumping structure, Moore *et al.* developed a Nd:YAG laser at 1123 nm with 1.7-W output power in a $TEM_{00}$ mode[1]. Despite the 1.1-$\mu$m lasers with diode-end-pumped scheme can achieve output with high beam quality; the output power was mostly limited at watt level. To scaling the output power, the diode-side-pumped structure was adopted by our group to generate high power 1112-nm lasers[20−22]. In 2010, Li *et al.* reported a 93.7-W 1112-nm laser with an $M^2$ factor of 17 by adopting diode-side-pumped gain module[21]. In 2011, we demonstrated a wavelength-tunable laser around 1.1 $\mu$m with a solid etalon inserted into the oscillator, which produced output powers of 75, 47, and 71 W at 1112, 1116, and 1123 nm and the corresponding $M^2$ factors were measured to be 14.5, 12, and 14, respectively[22]. Nevertheless, the high beam quality is a very important specification, especially for the nonlinear frequency conversion. In 2012, we reported a 30-W 1112-nm diode-side-pumped Nd:YAG laser with an $M^2$ factor of 1.2 through an optimized design of laser resonator. By using such light source as the fundamental laser, up to 1.5-W output power at 278-nm laser was obtained from FHG, which indicating a promising method to acquire high power UV lasers below 300 nm[20]. Recently, there has been a great interest in making reliable and compact 1112-nm laser with high output power and high beam quality. Former studies were mostly focusing on improving the characteristics of the laser oscillator. However, it is difficult to realize 1112-nm lasers with high power and high beam quality simultaneously by using a laser oscillator alone. The master-oscillator power-amplifier (MOPA)[23] system provides a feasible access to achieving high power laser with good beam quality. Meanwhile, the emission at 1112 nm is a low-gain line due to its much smaller stimulated emission cross-section than that of 1064-nm line[24], so it has a lower extracted efficiency in the amplifier compared with

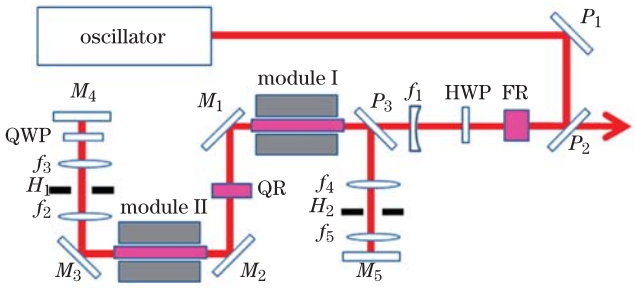


Fig. 1. Configuration of the two-stage four-pass MOPA laser system at 1112 nm. HWP: half-wave plate; QWP: quarter-ware plate.

 

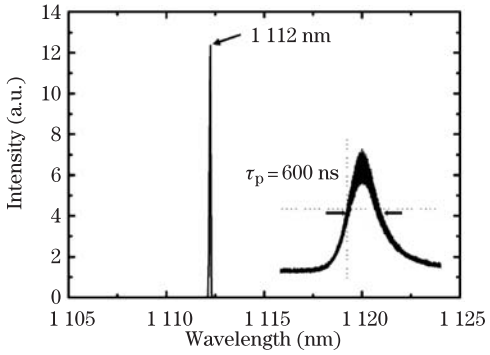


Fig. 2. Spectrum of the oscillator. Insert at right-down corner shows the expanded single pulse shape of the oscillator.

1064 nm. Conventionally, a complicated MOPA structure including seed laser for injection and multi-stage amplifiers are usually needed for the power scaling of the lasers at low-gain lines.

In this letter, a compact and stable scheme based on a two-stage four-pass 1112-nm Nd:YAG MOPA system is presented. The oscillator was an actively $Q$-switched Nd:YAG at 1112 nm and linearly polarized and near-diffraction-limited laser with an output power of 26 W. By employing two diode-side-pumped gain modules in the amplifier, we obtained an output power of 64-W Nd:YAG laser at 1112 nm, corresponding to an energy extraction efficiency of about 8 %. The beam quality at the highest output power was measured to be about $M^2$=2.85. Further, we employed a theoretical model that took into account the pulse temporal overlap and the inversion number dynamics to analyze the performance of the MOPA system.

The experimental configuration of the two-stage four-pass Nd:YAG 1112-nm MOPA system is shown in Fig. 1. The master-oscillator as a seed source was a 26-W two-rod Nd:YAG actively $Q$-switched (QS) linear polarized laser with a similar structure as our previous work in Ref. [20]. A solid etalon was inserted into the oscillator for line selection to guarantee the single wavelength laser operation at 1112 nm. The laser oscillator was operated at a repetition of 8 kHz with 200-$\mu$s pumping macropulse consisted 600-ns QS micropulses. The beam quality factor $M^2$ was measured to be 1.3.

In Fig. 1, $P_1$-$P_3$ were thin film polarizer with high reflection (HR) coated at 1112 nm in the perpendicular polarized (s-polarized) direction and high transmission (HT) coated in the parallel (p) direction with an incident angle of 45°. The focal length of lens $f_1$ was −200 mm and the focal length of $f_2$−$f_5$ was 100 mm. All spherical lenses were coated with HT at 1112 nm. Mirrors $M_1$−$M_3$ were coated with 45° HR at 1112 nm and HT at 1064 nm. Mirror $M_4$ and $M_5$ were coated with 0° HR at 1112 nm and HT at 1064 nm. An optical isolator consisted with a 45° Faraday rotator and a quarter-wave plate HWP was placed between $P_2$ and $P_3$, which not only prevented the return laser from the depolarizer and end-face reflection, but also acted as an optical switch which could release the four-pass amplified laser out from the amplifier. The seed laser beam was reflected twice by $P_1$ and $P_2$ and got matched with the rod size in the amplifier through the mode-matching lens $f_1$. The two Nd:YAG rods in the amplifier (Φ 3 ×72 (mm)) were doped with 0.6 at. -% concentration of $Nd^{3+}$ and HT coated at 1064 and 1112 nm on both end faces to reduce loss and suppress the parasite oscillation. Three quasi continuons wave (QCW) 808-nm laser diode (LD) arrays were symmetrically distributed around a rod in each module and provided a maximum pump power of 240 W at a repetition rate of 1 kHz. In the experiment, we used a digital pulse generator with double output channels to trigger the pumps for the oscillator and the amplifier, separately. To achieve high amplified power, we set an appropriate delay in the oscillator to accumulate enough energy in the amplifier. A 90° quartz rotator (QR) was placed between the two amplifier modules to compensate the thermally induced birefringence. Mirror $M_1$ and $M_2$ coated with HT at 1064 nm were arranged between the two modules for the sake of the suppression of 1064-nm laser. A pinhole and a telescope, denoted as ($f_2$, $H_1$, $f_3$) and ($f_4$, $H_2$, $f_5$), together acting as a spatial filter could ameliorate the beam quality. The diameter of the pinhole is about 1 mm, which can block most of the higher order modes without decreasing the power a lot. The QWP was used to switch the polarization state to the orthogonal direction after passing the modules twice. Eventually, the amplified laser pulse was switched out from $P_2$ after passing the amplifier four times.

Frantz *et al.*[25] established a theoretical model of the pulsed laser amplification by combining the photon transport equation and the laser rate equation. This widely adopted model agrees well with the single pass amplifier, nevertheless, it departs from the experimental results when dealing with multi-pass condition by using the single-pass output as the input of the next pass. Hirano *et al.*[26] reported a numerical description for double-pass amplifier considering different temporal overlap degrees with good accordance with their experimental output. Here, we adopt the analysis method reported by Pearce *et al.*[27] with the complete beam overlap assumption. We use $I_1^+$, $I_1^-$, $I_2^+$, $I_2^-$ to represent the irradiance of each pass, $I_1^+$ and $I_2^+$ were defined to be the forwards photon density and $I_1^-$ and $I_2^-$ to be the backwards ones. Taking into consideration the total photon flux as the sum of all the four-pass photon, the photon transport equation can be described as

$$\frac{\partial(I_1^+ + I_2^+)}{\partial t'} + c\frac{\partial(I_1^+ + I_2^+)}{\partial z'} = \sigma cn(I_1^+ + I_2^+), \qquad (1)$$

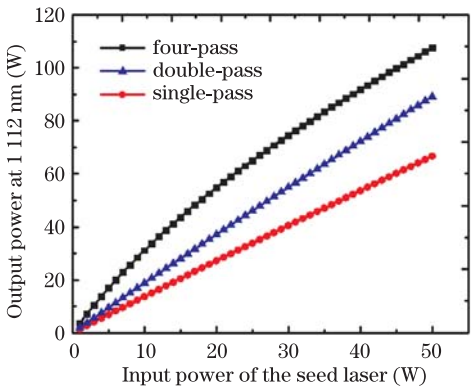


Fig. 3. (Color online) Simulation output of single (red), double (blue), and four pass (black) amplifiers versus seed injected power based on numerical model.

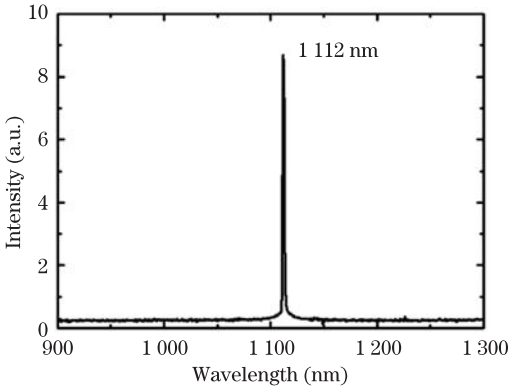


Fig. 4. Spectrum of the four-pass Nd:YAG MOPA laser.

$$\frac{\partial(I_1^- + I_2^-)}{\partial t'} + c\frac{\partial(I_1^- + I_2^-)}{\partial z'} = \sigma cn(I_1^- + I_2^-), \quad (2)$$

$$\frac{\partial n}{\partial t'} = -\frac{n\sigma}{h\upsilon}(I_1^+ + I_1^- + I_2^+ + I_2^-). \quad (3)$$

The output energy density $E_{\text{out}}$ and the inversion $N_{\text{TE}}$ can be derived as

$$E_{\text{out}} = \left(\frac{E_{\text{S}}}{M}\right)\ln\left[1 + (\exp\left(\frac{ME_{\text{in}}}{M}\right) - 1)\exp(M\sigma n)\right], \quad (4)$$

$$N_{\text{TE}} = -\left(\frac{1}{M\sigma}\right)\ln\left[1 - (1 - \exp(-M\sigma n))\right.$$
$$\left.\exp\left(-\frac{ME_{\text{in}}}{E_{\text{s}}}\right)\right], \quad (5)$$

where $E_{\text{S}}$ is the saturation fluency defined as $\frac{h\upsilon}{\sigma}$, $h\upsilon$ is the photon energy of 1112-nm laser, $\sigma$ is the efficient stimulated emission cross-section of 1112-nm line, $E_{\text{in}}$ is the input energy fluency and $N_{\text{TE}}$ is the length-integrated remaining inversion after amplification. Meanwhile, the number $M$=1, 2, 4 represents for the single, double and, four passing amplification scheme.

The spectrum of the oscillator and the expanded single pulse shape of the oscillator are presented in Fig. 2. It can be seen that only the wavelength centered at 1112 nm appears without other competitive lines. The pulse width of typical single micropulse is 600 ns. Based on this oscillator, we developed the four-pass MOPA laser system at 1112 nm.

To obtain larger effective gain volume and avoid strong diffraction, we arranged the injected seed beam size properly matched with the size of Nd:YAG rods using the plane-concave lens $f_1$ to prevent seed beam quality deterioration[26]. After being diverged through $f_1$, the seed laser injected into the gain modules and got single-pass amplified when departing from the Module $\prod$. While the pump power reached the maximum, an output of 35.5 W at 1112 nm was produced with a relatively low extraction efficiency of about 2%. Then we performed the double-pass scheme by making the laser make a round trip in the spatial filter and the QWP to get imaged into the gain modules with polarization state rotated by 90°. After passing through the two modules and the QR, the s polarized laser was reflected by $P_3$, where the double-pass amplification was completed. The output power of the double-pass scheme was measured behind $P_3$, which turned out to be 46 W with an extraction efficiency of about 4.2 %. The $M^2$ values was measured to be $M^2$=1.85 for the single pass amplification and $M^2$=2.21 for the double pass amplification, respectively. To sufficiently extract the energy stored in the gain medium, the other double-pass amplification was realized by placing the spatial filter ($f_4$, $H_2$, $f_5$) and $M_5$. When the second round trip in the gain medium was finished, the four-pass amplified laser with p direction polarization state eventually outputted from $P_2$. The output power was amplified to 64 W with an extraction efficiency of about 8 % after passing the amplifier four times. The second double-pass extracted efficiency was lower than that of the first double-pass owing to the gain decrease in the amplifier. With different input signal, the theoretical simulation of the output power with temporal overlap is illustrated in Fig. 3. The red, blue, and black lines represent the amplification simulation with single, double, and four times passing. The predicted output power for single-pass, double-pass, and four-pass schemes are 35, 48, and 67 W, respectively. The simulation with temporal overlap agreed well with the experimental results under our conditions. Accordingly, in further experiment, a seed laser with higher power or a pre-amplifier will be injected into the four-pass amplifier to achieve 100 W-level output, as can be expected from Fig. 2. We also calculate and see that when the seed laser increases over 100W, the power extracted from the four-pass amplifier will be saturated.

The characteristics of the four-pass configuration output laser were measured. The laser spectrum measured by an optical spectrum analyser (OSA AvaSpec-2048FT-SPU) was shown in Fig. 4, which indicates that only the wavelength centred at 1112 nm exists. As a reason accounting for the energy extraction degrading of 1112 nm laser, the parasitic oscillation and amplified spontaneous emission (ASE) of 1064 nm can easily be taken place in a multi-pass amplifier. It is noticeable that the arrangement of $M_1$ and $M_2$ was crucial in the effective suppression of the lasing at 1064 nm. We compared the spectrum of the output laser from the oscillator and the amplifier, as shown in Fig. 2, the centre wavelength and the linewidth did not change after amplification.

The amplified laser pulse profile was detected by using an oscilloscope with 1.5-GHz band-width and a fast silicon photoelectric detector. Figure 5 illustrates the experimental and simulated micropulse train and an

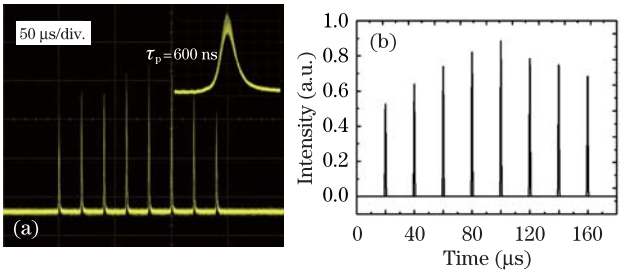


Fig. 5. Typical micropulse train shape of four-pass MOPA laser system. (a) Experimental pulse train; the insert at right-up corner shows the expanded single pulse shape; (b) simulated pulse train.

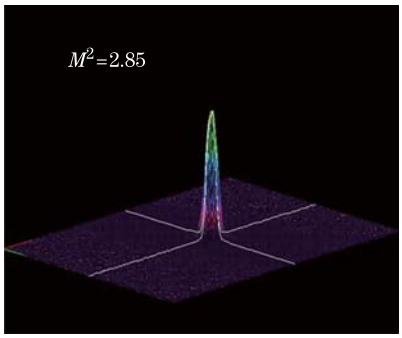


Fig. 6. 3D beam intensity distribution measured at the highest MOPA output power.

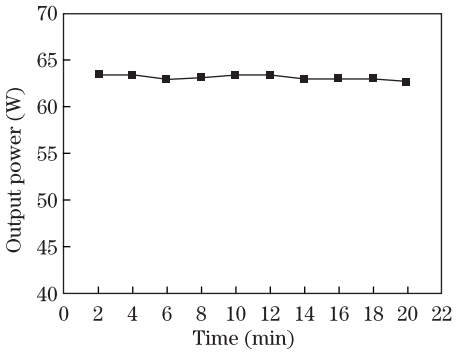


Fig. 7. Stability measurement of four-pass MOPA output power.

expanded single pulse profile of the 1112-nm laser. It can be seen from Fig. 5(a) that the micropulse width was about 600 ns. Besides, each single pulse in the pulse train was individually amplified. Obviously, the accumulation of the particles in the upper energy state is a dynamic process which was interfered by the QCW pumping, the emission of fluorescence, and the extraction of the injected laser. The interval of the injected $Q$-switched laser pulses was 20 $\mu$s, which was not enough for the accumulation of the population inversion to get equilibrium. In our calculation, the inversion reinforced in 20 $\mu$s exceeded the energy consumed by the amplification extraction and other effects, so the gain continued to increase within the pumping duration. That explains why the energy of every single pulse became stronger one after another. Nevertheless, when the pumping in the amplifier is over, the gain of amplification began to decrease and the later pulses in the pulse train became weaker. Similar pulse profile was obtained in our numerical simulation shown in Fig. 5(b). Meanwhile, we calculated the pulse width of a typical amplifier laser system was the same as the oscillator, which was testified in the experiment. The energy intensity of each micropulse in one macropulse pulse has changed as we discussed before, but the shape and pulse width did not change. The pulse width of each micropulse is 600 ns and the energy of single micropulse is around several millijoules. Since the peak power density of the seed laser in the Nd:YAG rod is more smaller than that of femtosecond and the nonlinear effect in our amplifier can be neglected.

The beam quality of the output laser was measured by a beam analyzer ($M^2$-200, Spiricon Inc.) at the maximum power. Figure 6 illustrates the three-dimensional (3D) beam intensity distribution of the amplified laser system. The beam quality factor $M^2$ was measured to be $M^2$=2.85. According to the beam profiles, the thermally induced birefringence was perfectly compensated so that there was no side lobe in the beam spot.

The output power stability of the amplifier was monitored at the full output. The measured result of the output power versus the time is shown in Fig. 7, which indicates the power fluctuation to be less than $\pm$0.75 % over 20 min. The performance of the MOPA laser suggests that the four-pass amplifier structure is a promising way in achieving high power high beam quality laser for the low gain lines.

In conclusion, we demonstrate a compact, high power, high beam quality LD side-pumped Nd:YAG four-pass MOPA laser system at 1112 nm. The MOPA laser delivers an output power of 64 W with the beam quality factor $M^2$ of 2.85. This is, to the best of our knowledge, the highest output power with such good beam quality reported to date for the 1112-nm Nd:YAG laser. Meanwhile, a theoretical model, including the temporal overlap and the dynamics of population inversion, is employed to analyze the performance of the MOPA system. The theoretical simulation is in fair agreement with the experimental data, and it suggests the possibility to achieve 100 W-level 1112-nm laser.

This work was supported by the State Key Program for Basic Research of China (No. 2010CB630706), the National High Technology Research and Development Program of China (No. 2011AA30202), and the Major Program of the National Natural Science Foundation of China (Nos. 51132008 and 61138004).

## References

1. N. Moore, W. A. Clarkson, D. C. Hanna, S. Lehmann, and J. Bösenberg, Appl. Opt. **38,** 5761 (1999).
2. Y. F. Chen and Y. P. Lan, Appl. Phys. B **79,** 29 (2004).
3. X. Guo, M. Chen, G. Li, B. Zhang, J. Yang, Z. Zhang, and Y. Wang, Chin. Opt. Lett. **2,** 402 (2004).
4. Z. Cai, M. Chen, Z. Zhang, R. Zhou, W. Wen, X. Ding, and J. Yao, Chin. Opt. Lett. **3,** 281 (2005).
5. J. Y. Huang, H. C. Liang, K. W. Su, H. C. Lai, Y. F. Chen, and K. F. Huang, Appl. Opt. **46,** 239 (2007).
6. S. S. Zhang, Q. P. Wang, X. Y. Zhang, Z. J. Liu, W. J. Sun, and S. W. Wang, Laser Phys. **19,** 2159 (2009).
7. S. S. Zhang, Q. P. Wang, X. Y. Zhang, Z. H. Cong, S. Z. Fan, Z. J. Liu, and W. J. Sun, Laser Phys. Lett. **6,** 864 (2009).
8. L. Chen, Z. Wang, S. Zhuang, H. Yu, Y. Zhao, L. Guo, and X. Xu, Opt. Lett. **36,** 13 (2011).
9. E. J. Zang, J. P. Cao, Y. Li, T. Yang, and D. M. Hong, Opt. Lett. **32,** 250 (2007).
10. C. Li, Y. Bo, F. Yang, Z. Wang, Y. Xu, Y. Wang, H. Gao, Q. Peng, D. Cui, and Z. Xu, Opt. Express **18,** 7923 (2010).
11. C. Y. Li, Y. Bo, Y. T. Xu, F. Yang, Z. C. Wang, B. S. Wang, J. L. Xu, H. W. Gao, Q. J. Peng, D. F. Cui, and Z. Y. Xu, Opt. Commun. **283,** 2885 (2010).
12. J. Gao, X. J. Dai, L. Zhang. H. X. Sun, and X. D. Wu, Appl. Phys. B **111,** 407 (2013).
13. N. V. Kravtsov, V. V. Firsov, and P. P. Pashinin, Quantum Electron. **29,** 778 (1999).

14. Y. F. Chen, Y. P. Lan, and S. W. Tsai, Opt. Commun. **234,** 309 (2004).
15. F. Q. Jia, Q. Zheng, Q. H. Xue, and Y. K. Bu, Opt. Laser Technol. **38,** 569 (2006).
16. Q. Zheng, Y. Yao, D. Qu, K. Zhou, Y. Liu, and L. Zhao, J. Opt. Soc. Am. B **26,** 1939 (2009).
17. Z. Wang, Q. Peng, Y. Bo, J. Xu, S. Xie, C. Li, Y. Xu, F. Yang, Y. Wang, D. Cui, and Z. Xu, Appl. Opt. **49,** 3465 (2010).
18. Z. Wang, F. Yang, S. Xie, Y. Xu, J. Xu, Y. Bo, Q. Peng, J. Zhang, D. Cui, and Z. Xu, Appl. Opt. **51,** 4196 (2012).
19. Z. C. Wang, J. L. Xu, Y. Bo, Q. J. Peng, S. Y. Xie, Y. T. Xu, F. Yang, J. Y. Zhang, D. F. Cui, and Z. Y. Xu, Laser Phys. **22,** 142 (2012).
20. Z. Wang, F. Yang, G. Zhang, Y. Bo, S. Liu, S. Xie, Y. Xu, N. Zong, F. Li, B. Liu, J. Xu, Q. Peng, J. Zhang, D. Cui, Y. Wu, and Z. Xu, Opt. Lett. **37,** 12 (2012).
21. C.Y. Li, Z. C. Wang, Y. T. Xu, F. Yang, B. S. Wang, H. W. Gao, Y. Bo, Q. J. Peng, D. F. Cui, and Z. Y. Xu, Laser Phys. **20,** 1572 (2010).
22. Z. Wang. Y. Bo. S. Xie. C. Li. Y. Xu. F. Yang. J. Xu. Q. Peng. J. Zhang. D. Cui. and Z. Xu, Appl. Phys. B **104,** 45 (2011).
23. S. Singh, R. G. Smith, and L. G. V. Uitert, Phys. Rev. B **10,** 2566 (1974).
24. S. Li, X. Ma, H. Li, F. Li, X. Zhu, and W. Chen, Chin. Opt. Lett. **11,** 071402 (2013).
25. L. M. Frantz and J. S. Nodvik, J. Appl. Phys. **34,** 2346 (1963).
26. Y. Hirano, N. Pavel, S. Yamamoto, Y. Koyata, and T. Tajime, Opt. Commun. **170,** 275 (1999).
27. S. Pearce, C. L. M. Ireland, and P. E. Dyer, Opt. Commun. **255,** 297 (2005).